An assessment of the permeation enhancer, 1-phenyl-piperazine (PPZ), on paracellular flux across rat intestinal mucosae in Ussing chambers

V. A. Bzik & D. J. Brayden

Corresponding author:
D. J. Brayden: School of Veterinary Medicine and Conway Institute, University College Dublin, Belfield, Dublin 4, Ireland. Tel: +35317166013; fax: +3531 7166214; email: david.brayden@ucd.ie

V. A. Bzik: School of Veterinary Medicine and Conway Institute, University College Dublin, Belfield, Dublin 4, Ireland.

Running head: Phenyl piperazine promotes intestinal permeation *in vitro*

ABSTRACT

Purpose: 1-phenyl piperazine (PPZ) emerged from a Caco-2 monolayer screen as having high enhancement potential due to a capacity to increase permeation without significant toxicity. Our aim was to further explore the efficacy and toxicity of PPZ in rat ileal and colonic mucosae in order to assess its true translation potential.

Methods: Intestinal mucosae were mounted in Ussing chambers and apparent permeability coefficient (Papp) values of [^{14}C]-mannitol and FITC-dextran 4 kDa (FD-4) and transepithelial electrical resistance (TEER) values were obtained following apical addition of PPZ (0.6-60 mM). Exposed issues were assessed for toxicity by histopathology and lactate dehydrogenase (LDH) release. Mucosal recovery after exposure was also assessed using TEER readings.

Results: PPZ reversibly increased the Papp of both agents across rat ileal and distal colonic mucosae in concentration-dependent fashion, accompanied by TEER reduction, with acceptable levels of tissue damage. The complex mechanism of tight junction opening was part mediated by myosin light chain kinase, stimulation of transepithelial electrogenic chloride secretion, and involved activation of 5-HT_4 receptors.

Conclusions: PPZ is an efficacious and benign intestinal permeation enhancer in tissue mucosae. However, its active pharmacology suggest that potential for further development in an oral formulation for poorly permeable molecules will be difficult.

KEY WORDS: phenyl piperazine; intestinal permeation enhancers; Ussing chambers; oral peptides; epithelial tight junctions

LIST OF ABBREVIATIONS

1-phenyl piperazine (PPZ)

Apparent permeability coefficient (Papp)

Transepithelial electrical resistance (TEER)

Lactate dehydrogenase (LDH)

Fluorescein isothiocyanate (FITC)

FITC-dextran (FD)

Forskolin (FSK)

Krebs-Henseleit solution (KH)

3-(4,5-dimethylthiazol-2-yl)-2,5-diphenyltetrazolium bromide) tetrazolium (MTT)

1-(5-chloronaphthalene-1-sulfonyl)-1H-hexahydro-1,4-diazepine] (ML9)

3-isobutyl-1-methyl-xanthine (IBMX)

Myosin light chain kinase (MLCK)

Protein kinase A (PKA)

Protein kinase C (PKC)

Cystic fibrosis transmembrane regulator (CFTR)

Sodium/potassium/chloride cotransporter (Na/K/2Cl)

Sodium salt of capric acid (C_{10})

Diketofumaryl piperazine (DKFP)

Short circuit current (Isc)

Hank's balanced salt solution (HBSS)

INTRODUCTION

1-phenyl piperazine (PPZ, CAS number 92-*54-6; Fig. 1*) was identified as a potentially efficacious epithelial permeability enhancer with low cytotoxicity in a Caco-2 monolayer screening study of 51 putative agents (1). Compared to other enhancers, 0.1% PPZ had the highest overall potential (0.86/1.00) as efficacious enhancers using the apparent permeability coefficients (Papp) achieved with [^{3}H]-mannitol and 70 kDa dextran across Caco-2 monolayers. PPZ (0.1%) showed one of the largest decreases in monolayer TEER normalized to that of 1% Triton®-X-100, while at the same time it had little effect on MTT production, indirect evidence of a high enhancement potential *in vitro*. Moreover, fluorescent microscopy images suggested that 0.1% PPZ promoted the paracellular pathway, as indicated by calcein measurements in Caco-2 cells (2). A recent study (3) further tested the mechanism of action of 13 PPZ-related derivatives andconcluded that an apical side buffer pH of 8.7-9.6 was conferred by piperazine enhancers in Caco-2 monolayer studies, suggesting a role for pH-dependent molecular parameters. To our knowledge however, no study has further examined whether PPZ enhances permeation in less reductionist intestinal tissue models, nor what the mechanism of stimulating paracellular flux increase might be.

Designation of “non-toxic” to an agent on the basis of two cytotoxicity assays in Caco-2 cells might be somewhat premature, as the MTT and LDH release assays have limitations and there is limited predictive correlation between cytotoxicity data seen in Caco-2 cells and that of less reductionist models, or indeed with *in vivo*. Moreover, piperazine structures are associated with active pharmacology: piperazine citrate was developed in the 1950s as a treatment for roundworm and threadworm infections, by inducing paralysis via GABA receptor antagonism

(4). PPZ and piperazine derivatives are also ligands for dopamine (D_2)-like, 5-HT_{1A} and 5-HT_4 receptors (5, 6); some exhibit antidepressant properties by inhibiting neurokinin receptors (7), while others are also used in the treatment of schizophrenia (8) and motion sickness (9). Up to 10 mg of 5-HT is stored in enterochromaffin cells in the human intestine, accounting for 60-90% of the overall 5-HT in the body (10), and when stimulated, the EC cells release 5-HT to activate receptors on adjoining nerves (11). 5-HT impacts gastrointestinal motility (12), colonic transit (13) and enterocyte epithelial electrogenic ion secretion (14). After stimulation, epithelial cells and platelets reabsorb 5-HT from the interstitial space through the serotonin-selective reuptake transporter (SSRT) at the base of crypts or in the basement membrane (15), thereby removing luminal 5-HT to dampen further mucosal effects (16). It causes an increase in short circuit current (Isc) via 5-HT_4 receptor activation in rat colonic mucosae with an EC_{50} of 4 µM (17, 18), so these receptors are functional in isolated tissue mucosae and may respond to low concentrations of agonists including piperazines, a pathway that cannot accurately be probed in Caco-2 monolayers due to variable receptor expression and unreliable Isc responses. Therefore, the extensive pharmacology of piperazines if demonstrated in relevant intestinal models, could mitigate against their development as oral permeability enhancers. On the other hand, diketofumaryl piperazine (DKFP), another piperazine derivative, is a solubilizing non-active excipient in MannKind Corporation's Technosphere™ dry powder delivery system, which was approved in 2014 for pulmonary delivery of insulin to Type I and II diabetics (Afrezza®) (19). There has been no data published to suggest that DKFP has active pharmacology in the lung, whatever about the intestine.

The study aims were to therefore to determine whether PPZ might increase paracellular permeability in non-cytotoxic fashion across isolated rat intestinal mucosae mounted in Ussing chambers, and also to verify if the Caco-2 monolayer screening of this putative enhancer was predictive. Secondly, we investigated whether myosin light chain kinase inhibitors and 5-HT_4 antagonists could inhibit PPZ-induced permeability across Caco-2 monolayers and rat intestinal tissue mucosae. We confirmed that PPZ increases paracellular flux in concentration-dependent fashion across rat intestinal mucosae, and that *selected* enhancing concentrations are indeed non-cytotoxic, but suggest that the mechanism of action at the tight junction is multi-factorial, highly complex, and involves epithelial 5-HT receptor activation.

MATERIALS AND METHODS

Intestinal tissue preparation for Ussing chamber studies

Studies carried out were in accordance with the UCD Animal Research Ethics Committee protocol, AREC-14-28 Brayden, and were in adherence with the "*Principles of Laboratory Animal Care*," (NIH Publication #85-23, revised in 1985). Male Wistar rats (250-300 g; Charles River, UK) were housed in the Biomedical Facility in University College Dublin (UCD) under controlled environmental conditions with 12:12 light: dark cycles, as well as with access to tap water and standard laboratory chow *ad lib*. Rats were euthanized by stunning followed by cervical dislocation. Ileal or colonic mucosae were removed and placed into freshly oxygenated Krebs-Henseleit buffer (KH). Excised intestinal epithelial tissue with intact *lamina propria* was dissected free of underlying smooth muscle according to previous descriptions (e.g. 20). Mucosae were pinned between pre-equilibrated Ussing chamber halves (World Precision

Instruments, WPI, UK) with circular diameters of 0.63 cm^2. 5 mL KH was added bilaterally and chamber fluids were oxygenated using a gas-lift system with 95% O_2/5% CO_2 at 37°C. Each chamber half had voltage and current electrodes connected to a voltage clamp apparatus (EVC4000; WPI, UK) via a pre-amplifier. Silver/silver chloride (Ag/AgCl) electrodes were prepared by heating 3 M KCl with 3% agar and cooled in plastic casing. The potential difference (PD; mV) was measured across the mucosa in an open circuit configuration. When the voltage was clamped to 0 mV, the short circuit current (Isc; $\mu A/cm^2$) was determined and transepithelial electrical resistance (TEER; $\Omega.cm^2$) was determined by Ohm's Law.

Cultured Caco-2 cell monolayers

Caco-2 cells (Passage 55-60) were obtained from ECACC and grown in 75 cm^2 flasks containing DMEM supplemented with 10% v/v heat-inactivated fetal calf serum, 1% v/v penicillin/streptomycin solution, 1% v/v non-essential amino acids and 1% v/v L-glutamine in a humidified incubator gassed with 95% O_2/5% CO_2, at 37°C. Viability was determined by the exclusion of trypan blue with the Vi-CELL™ Series Cell Viability Analyzer (Beckman Coulter). Caco-2 cells were seeded at a density of 5 x 10^5 cells/well and grown for 21 days on 12mm polycarbonate Transwell® supports with a 0.4 µm pore size (#3401; Corning Costar Corp., USA) (21). Transepithelial electrical resistance (TEER; $\Omega.cm^2$) was determined throughout the experiment using an EVOM® voltohmmeter with chopstick-type electrodes (WPI, UK). Percentage reduction in TEER was measured relative to TEER at the start of the experiment.

Paracellular fluxes induced by PPZ across monolayers and tissue mucosae

Monolayer fluxes were measured over 120 min in HBSS supplemented with HEPES (25 mM) and

glucose (11 mM). Following 20 min equilibration, PPZ (0.6-60 mM) was added to the apical side of the Ussing chamber in the presence of the paracellular flux markers, [^{14}C]-mannitol (0.1 uCi/mL) and FITC-4000 (FD-4; 2.5 mg/mL). For Caco-2 monolayers, FD-40 and FD-70 were also used. In monolayers, a 10x solution was prepared before added to the 0.5 mL apical bath. Basolateral samples (200 µL) were taken every 20 min for 120 min and replaced with fresh KH/HBSS. Samples were mixed with 3 mL of scintillation fluid and analyzed on a liquid scintillation analyzer (Packard Tricarb 2900 TR). The apparent permeability coefficient (Papp, cm/s) was determined by the following equation: $Papp = dQ/dt\ (1/A*C_0)$, where dQ/dt was the transport rate (mol/s); A was the surface area (0.63 cm^2 for intestinal mucosae; 1.1 cm^2 for monolayers); C_0 was the initial concentration in the donor compartment (mol/mL) (21).

Effects of MLCK inhibitors on PPZ-induced paracellular permeability enhancement

Myosin light chain kinase (MLCK) inhibitor including 1-(5-chloronaphthalene-1-sulfonyl)-1H-hexahydro-1,4-diazepine] (ML9, Calbiochem, UK) can prevent phosphorylation of MLCK (22). To further determine the mechanisms by which PPZ may function, monolayers and rat colonic mucosae were pre-treated with ML9 for 20 min prior to addition of apical addition of PPZ and, following fluxes of 120 min, the Papp of [^{14}C]-mannitol and FD-4 were calculated.

Effect of 5-HT$_4$ receptor inhibition on PPZ-induced fluxes *in vitro* and *ex vivo*

5HT hydrochloride (5-15 µM) was added either apically or basolaterally to monolayers or mucosae before addition of [^{14}C]-mannitol and FD-4. The resulting Papp was calculated for [^{14}C]-mannitol and FD-4. Selective 5-HT$_4$ antagonists, SB-204070 (10 µM, Sigma-Aldrich, Ireland) and GR11808 (1 µM, Sigma-Aldrich) (23), were applied bilaterally 20 min prior to the apical side addition of PPZ and 5-HT to monolayers and colonic mucosae.

Effect of PPZ on cAMP levels in Caco-2 cells and colonic mucosae

When Caco-2 reached 70-80% confluence, they were trypsinized with trypsin-EDTA (1X; Gibco, Ireland) and seeded onto collagen (5 µg/cm^2) coated 24-well plates at a density 1 x 10 ^{x6} cells/mL. On day 3, cells were washed with serum free media (SFM) and then incubated with fresh SFM, supplemented with 1mM of the phosphodiesterase inhibitor, 3-isobutyl-1-methyl-xanthine (IBMX, Calbiochem) in a humidified incubator with 95% O_2/5% CO_2, at 37°C for 60 min. PPZ (0.6-60 mM) or the adenylate cyclase activator, forskolin (FSK, 10 µM) were then added for 15 min and then aspirated. The cells were trypsinized and DMEM was added to inactivate the trypsin. The cells were then centrifuged at 10,000 rpm for 10 min and washed 3 times with cold PBS. The pellet was resuspended in cell lysis buffer 5 (1x) at a concentration 1 x 10^7 cells/mL and stored at -20°C. A freeze/thaw cycle was performed to ensure total cell lysis. The lysate was then centrifuged at 600 x g for 10 min at 4°C to remove cellular debris and the supernatant was stored at -20°C. Rat colonic mucosae were also equilibrated for 45 min before the basolateral addition of PPZ (0.6-60 mM) and FSK (10 µM) treatments in the presence of IBMX (1 mM). After 15 min, the mucosae were removed from the chamber and snap-frozen in liquid nitrogen. The tissue was homogenized in cell lysis buffer 5 (1x) and stored at -20°C. A

freeze/thaw cycle was performed before being centrifuged at 600 x g for 10 min at 4°C and stored at -20°C. The supernatants from Caco-2 cells and tissue mucosae were tested for the capacity to induce cAMP production in duplicate following the manufacturer's instructions (Parameter™ cAMP assay; Catalogue number KGE002; R&D Systems) (24).

Cytotoxicity assay in Caco-2 cells and intestinal mucosae

The viability of Caco-2 cells treated with PPZ was determined by the MTT assay (25). Cells were seeded at a density of 1 x 10^5 cells/mL in 96-well plates for 24 h. Fresh DMEM was applied and allowed to equilibrate before PPZ (60 µM-60 mM) or Triton® X-100 (0.1% v/v) were added. Plates were then placed into a humidified incubator with 95% O_2/5% CO_2, at 37°C for 1 h or 24 h exposure. The LDH assay was also carried out for PPZ-treated rat mucosae as previously described (26). Ileal and colonic mucosae were mounted in Ussing chambers for 120 min and samples of apical bathing solution (200 µL) was removed at 0, 60 and 120 min and replaced with fresh KH. Samples were mixed with 200 µL TOX-7 for 30 min and assayed.

Confocal and light microscopy

Filter-grown Caco-2 monolayers were treated with PPZ (0.6 mM) for 20 min, washed 3 times with (PBS and fixed with paraformaldehyde (4% w/v) in PBS for 20 min. The monolayers were then washed 3 times with PBS and permeabilized with Triton® X-100 (0.1% v/v) in 5% w/v normal goat serum (NGS) in PBS for 60 min. After an additional 3 washes with PBS, monolayers were stained with primary antibody of mouse anti-claudin-2 (1:200; Zymed Laboratories, USA) in 5% NGS for 60 min, before being washed a further 3 times with PBS. The monolayers were

stained with a secondary antibody of Alexa Fluor® 568 anti-mouse IgG (1:200; Zymed Laboratories) and FITC-phalloidin in 5% NGS for 60 min before being washed 3 times with PBS and incubated with 4',6-diamidino-2-phenylindole (DAPI; 1:10,000) for 10 min. The monolayers were washed with fresh PBS to remove any extra stain. The monolayers were then excised from inserts and mounted onto glass slides with Vectrashield® mounting medium (Vector Laboratories Ltd., UK) and the edges were sealed with clear nail varnish and stored at -20°C. Confocal microscopy was preformed on a Zeiss LSM 510 Meta using LSM5 acquisition software (Carl Zeiss Inc.) with a 543 nm filter (rhodamine), a 488 nm filter (FITC) and a 364 nm filter (DAPI). For light microscopy, rat ileal and rat colonic mucosae were treated apically with PPZ (0.6-60 mM) for 120 min. Mucosae was removed from the chambers and placed into 10% v/v buffered formalin and then embedded in paraffin wax. Tissue sections were mounted on adhesive coated slides, and stained with H&E. The slides were visualized under a light microscope (Labophot-2A; Nikon, Japan) and images taken with a high-resolution camera (Micropublisher 3.3 RTV; QImaging, Canada) and Image-Pro® Plus version 6.3 (Media Cybernetics Inc., USA) acquisition software.

Statistical analysis

Statistical analysis was carried out using Prism-5® software (GraphPad®, USA). Unpaired Student's t-tests and ANOVA were used for single and group comparisons respectively. Results are given as mean ± SEM. A significant difference was deemed present if $P<0.05$.

RESULTS AND DISCUSSION

PPZ causes an increase in paracellular flux markers across *in vitro* and *ex vivo* models

The basal Papp of [^{14}C]-mannitol, FD-4, FD-40 and FD-70 was 7.8 ± 0.2 x 10^{-8} cm/s (n=7), 5.1 ± 0.4 x 10^{-8} cm/s (n=12), 3.2 ± 0.3 x 10^{-8} cm/s (n=3), and 2.5 ± 0.5 x 10^{-8} cm/s (n=4), respectively across Caco-2 monolayers. The mean basal TEER of monolayers was 1905 ± 26 Ω.cm2 (n=13). The basal Papp of the flux markers within previously published ranges for Caco-2 monolayers (27, 28), as were the TEER values (29) Apical addition of PPZ (0.6-60 mM) caused an increase in Papp of each of the four markers across monolayers (Fig. 2a, b). The basal Papp across rat ileal mucosae was 7.4 ± 1.3 x 10^{-7} cm/s (n=5) and 6.5 ± 0.8 x 10^{-7} cm/s (n=4) for [^{14}C]-mannitol and FD-4, respectively. The mean basal TEER of ileal mucosae was 53 ± 3 Ω.cm^2 (n=10) and both the basal fluxes and TEER values were within acceptable limits (30-32). The basal distal colonic mucosae TEER was 147 ± 4 Ω.cm2 (n=61), while the basal Papp across distal colonic mucosae was 5.7 ± 0.6 x 10^{-7} cm/s (n=9) and 4.7 ± 0.7 x 10^{-7} cm/s (n=10) for [^{14}C]-mannitol and FD-4 respectively, values also within the acceptable range (26, 30). Apical addition of PPZ (6-60 mM) increased flux of [^{14}C]-mannitol and FD-4 across rat ileal and distal colonic mucosae over 120 min (Fig. 3a, b), accompanied by concentration-dependent reductions in TEER in both tissue types (Fig. 3c, d). Thus, an inverse relationship was present between the increased fluxes of the paracellular markers and reduction in TEER values in monolayers, as well as across ileal, and distal colonic mucosae.

Apically-added PPZ at a lower concentration of 0.6 mM caused an increase in the Papp for both flux markers in rat distal distal colon, but only for FD-4 in rat ileum (Fig. 3a). Importantly, PPZ (0.6 mM) caused an 8-fold increase in Papp of [^{14}C]-mannitol across distal colonic mucosae, but

was without effect on the Papp across proximal colonic mucosae ($P<0.001$), so all colonic studies within refer to the former. While *basolateral* addition of PPZ (0.6-6 mM) had no effect on the [^{14}C]-mannitol Papp across ileal or colonic mucosae, a concentration of 60 mM added to that side increased the Papp, but this was associated with histological damage (data not shown). To test recovery of monolayers exposed to 0.6-60 mM PPZ, the apical reservoir buffer containing PPZ were replaced with with KH and the TEER recovered over 24 h for 0.6 and 6mM, but not for 60 mM. (Fig. 4). In parallel studies in colonic tissue, apical side additions of PPZ again reduced TEER over 20 min and, following incubation in fresh KH for 2h, TEER partially recovered to 80% maximum TEER (versus 35%, without wash-out) and 75% maximum TEER (versus 30%, without washout) in the respective cases of 0.6 and 6 mM, but not at all to 60 mM where it remained at just 10% maximum TEER throughout irrespective of wash-out (n=4 each group, data not shown).

PPZ activates apical 5-HT$_4$ receptors and increases intracellular cAMP

It was hypothesized that the mechanism of action of PPZ in enhancing paracellular permeability in intestinal epithelial *in vitro* models was via an action at 5-HT$_4$ receptors in plasma membranes of Caco-2 monolayers (33) and intestinal epithelia (34). Bilateral pretreatment of monolayers for 20 min with the selective 5-HT$_4$ antagonists, SB-204070 (10 µM) and GR11808 (1 µM) caused a reduction in PPZ (0.6 mM)-induced increase in the Papp of [^{14}C]-mannitol (Fig. 5a). At higher concentrations of PPZ (6-60 mM) however, SB-204070 had no effect. In contrast, GR11808 reduced the PPZ (6-60 mM)-induced permeability at these higher PPZ concentrations, although Papp values were still higher than those for untreated monolayers (data not shown).

In rat distal colonic mucosae, pretreatment with bilateral SB-204070 and GR11808) also caused a reduction in PPZ (0.6, 6 and 60 mM)-induced Papp of [14C]-mannitol (Fig. 5b). Due to limited availabilities of 5-HT_4 antagonists, these experiments were not repeated in rat ileal mucosae. These data suggest that PPZ opens tight junctions in part by activation of 5-HT_4 receptors on the apical membranes of both monolayers and colonic tissue.

Intracellular cAMP concentrations in Caco-2 cells after 15 min exposure to PPZ (60 μM-60 mM) were increased (Figure 6a), although levels were lower than the maximal effects stimulated by the positive control, FSK (10 μM). Basal cAMP levels were 26.3 ± 1.8 (n=4) and 20.5 ± 0.9 pmol/mg (n=4) for Caco-2 cells and rat colonic mucosae, respectively. Basolateral addition of FSK (10 μM) caused a maximal increase in intracellular cAMP after 15 min in both Caco-2 and colonic mucosae, Δ 26.1 ± 0.9 (n=4) and Δ 21.4 ± 0.5 pmol/mg (n=4), respectively. In rat colonic mucosae, apical addition of PPZ (6-60 mM) also caused increases in intracellular cAMP after 15 min exposure (Fig. 6b). Agents including FSK elevate intracellular cAMP and are well-known to induce electrogenic Cl^- and H_2O secretion across intestinal tissue mucosae, increasing epithelial tight junction permeability in parallel (35). We confirmed that apical addition of PPZ caused concentration-dependent increases in Isc across colonic mucosae in the concentration range that enabled increased flux of paracellular markers and reductions in TEER (Fig. 6c); effects from apical addition were more efficacious than basolateral, confirming the importance of apical side presentation to 5HT_4 - and possibly other receptors. Furthermore, 20 min pre-treatment with the loop diuretic and inhibitor of the basolateral Na/K/2Cl cotransporter, bumetanide (100 μM), followed apical PPZ (0.6-60 mM) reduced the capacity of PPZ to

stimulate the Papp of [^{14}C]-mannitol across rat distal colonic mucosae over 120 min (Table 1). Therefore this data suggests that PPZ may activate $5HT_4$ G-protein coupled receptors, which in turn regulates the Na/K/2Cl cotransporter via adenylate cyclase mediated production of cAMP ultimately to stimulate electrogenic chloride secretion and to open intestinal epithelial tight junctions.

PPZ paracellular transport is facilitated by MLCK in monolayers and colonic mucosae

The mechanism of action by which PPZ increased permeability across intestinal tissue may involve multiple pathways, therefore several inhibitors were used to examine regulated enzymes pertaining to tight junction opening. ML9 is a reversible competitive inhibitor of MLCK (K_i: 3.8 μM), PKA (K_i: 32 μM), and PKC (Ki: 54 μM) (36). Pre-incubation with ML9 (10 μM), reduced the Papp of [^{14}C]-mannitol and FD-4 in PPZ-stimulated Caco-2 monolayers (Fig. 7a) and rat distal colonic mucosae (Fig 7b). Therefore it appears that MLCK is involved in the intracellular mechanism of PPZ-induced tight junction openings.

PPZ effects expression of F-actin and claudin-2 in Caco-2 monolayer tight junctions

Confluent monolayers stained with F-actin showed a typical “chicken wire” conformation around the periphery of each cell (Fig. 8a). Apical addition of PPZ (0.6 mM) for 20 min caused a decrease in F-actin staining around the cell and an increase staining of G-actin in the cytoplasm (Fig. 8b). Monolayers stained with claudin-2 antibodies showed little or no expression in untreated monolayers (Fig. 8c). Following PPZ (0.6 mM) addition however, increased claudin-2 expression was observed between treated cells (Fig. 8, d), indicative of increase paracellular

permeability (37). This suggests that PPZ alters tight junction protein expression as well as F-actin localization in treated monolayers at concentrations known to increase paracellular permeability.

Concentration-dependent toxicity of PPZ *in vitro* and *ex vivo*: MTT, LDH and histology

The MTT assay was used to examine both acute (1 h) and chronic (24 h) exposure to PPZ in Caco-2 cells. There was a significant reduction in cell viability when PPZ (6-60 mM) was added to Caco-2 cells for these time periods (Fig. 9a, b). However, this decrease was much less than damage caused by the addition of Triton® X-100 (0.1% v/v). Nevertheless, after 60 min of PPZ (6 mM) exposure, the majority of cells were still viable (73.7 ± 5.1%), but this decreased to almost half after 24 h (57.5 ± 9.5%). PPZ (up to 0.6 mM) however was relatively non-cytotoxic to Caco-2 cells up to 24 h, the same concentration that could enhance flux of paracellular flux markers. In rat ileal (Fig. 9c) and colonic (Fig. 9d) mucosae mounted in Ussing chambers for 120 min, there was no increase in LDH release at concentrations of PPZ of 0.6-6 mM, however 60 mM PPZ induced LDH release comparable to Triton® X 100, suggesting a toxic effect at this concentration. Light microscopy of rat ileal and colonic mucosae exposed to PPZ for 120 min was examined using H&E staining (Fig. 10). There was an increase in epithelial cell damage with high concentrations of PPZ (6 mM) (Fig. 10 c, f) compared to lower concentration of 0.6 mM (Fig. 10 b, e) in both ileal and colonic mucosae. Lower concentrations of PPZ (0.6 mM) induced little damage in either ileal or colonic tissue compared to controls (Fig. 10 a, d).

SUMMARY AND CONCLUSIONS

345 Previous work using Caco-2 cells indicated that PPZ was in the top tier of a screen of molecules
346 that displayed high permeation enhancer efficacy and low cytotoxicity (1,2) with direct
347 evidence for induced tight junction openings (2). Here, we confirmed and expanded on some
348 of these data using isolated rat intestinal tissue mucosae and provide further insight into the
349 mechanism of action of PPZ on intestinal epithelia, as well as information on its pharmacology
350 and toxicology. Firstly, PPZ induced flux of several paracellular flux markers across Caco-2
351 monolayers and rat ileal and distal colonic mucosae models. Secondly, by comparing PPZ to
352 other permeation enhancers also tested in isolated rat intestinal tissue mucosae, we can
353 conclude that its efficacy is on a par with some of the gold standard enhancers in clinical trials
354 including C_{10}, and palmitoyl carnitines, both thought to act in part by opening tight junctions via
355 intracellular-mediated mechanisms, driven by initial plasma membrane perturbation and
356 fluidization (reviewed in (38)). A combination of MTT assay in Caco-2 cells, LDH release from
357 intestinal tissue, reversibility of TEER reductions upon PPZ removal in monolayers and tissue
358 mucosae, and histology of mucosal sheets following PPZ exposure suggested that
359 concentrations up to 6mM were non-toxic in these bioassays. As with medium chain fatty acid
360 salts, there is a concentration window in which PPZ induces increased paracellular flux without
361 significantly damaging cells and tissues. Recently, Lamson et al (3), examined a set of
362 hydrocarbon-substituted piperazine derivatives as permeation enhancers in Caco-2 monolayers
363 and an important factor was that effective non-cytotoxic ones altered the apical-side HBSS pH
364 to 9.2-9.6, thereby causing permeability enhancement beyond what was expected from pH
365 changes alone. Alkaline pH induction of the apical-side buffer, at least *in vitro*, appears

366 therefore to contribute in part to the tight junction-opening effects of piperazine-related
367 structures.
368
369 Examination of the true translational potential of any putative candidate also involves study of
370 its intestinal pharmacology, which ideally should be minimal. It was hypothesized that the
371 specific mechanism of action of PPZ in enhancing paracellular permeability might be through 5-
372 HT_4 receptors present on the apical membrane of Caco-2 cells and intestinal epithelia. Apical
373 addition of PPZ activated 5-HT_4 receptors in monolayers and tissue mucosae (inhibited in part
374 by two antagonists) resulting in a cascade of events. These included an increase in intracellular
375 cAMP, stimulation of the MLC pathway, activation of the basolateral Na/K/2Cl cotransporter,
376 ultimately leading to an increase in transepithelial electrogenic chloride secretion (i.e. Isc
377 increase) linked to tight junction modulation (i.e. bumetanide-sensitivity). A cartoon is
378 provided to summarize these pathways (Fig. 11). In conclusion, the clinical use of PPZ as a
379 potential oral drug permeation enhancer is therefore likely to be limited by its multiple
380 mechanisms on intestinal epithelial ion transport function, as well as by its interaction with the
381 physiologically-important enteric 5-HT system.
382
383
384
385
386
387

ACKNOWLEDGMENTS AND DISCLOSURES

This study was co-funded by Science Foundation Ireland grant 07/SRC B1144. V.A. Bzik was recipient of a UCD *Ad Astra* Scholarship. An abstract of this study was presented at the CRS Annual Meeting; Copenhagen, Denmark (2009).

REFERENCES

1. Whitehead K, Karr N, Mitragotri S. Safe and effective permeation enhancers for oral drug delivery. Pharm Res. 2008;25(8):1782-1788.

2. Whitehead K, Mitragotri S. Mechanistic analysis of chemical permeation enhancers for oral drug delivery. Pharm Res. 2008;25(6):1412-1429.

3. Lamson NG, Cusimano G, Suri K, Zhang A, Whitehead KA. The pH of piperazine derivative solutions predicts their utility as transepithelial permeation enhancers. Mol. Pharm. 2016; 13: 578-585.

4. Martin RJ. Electrophysiological effects of piperazine and diethylcarbamazine on *Ascaris suum* somatic muscle. Br J Pharmacol. 1982;77(2):255-265.

5. Neves G, Menegatti R, Antonio CB, Grazziottin LR, Vieira RO, Rates SM, et al. Searching for multi-target antipsychotics: discovery of orally active heterocyclic N-phenylpiperazine ligands of D2-like and 5-HT1A receptors. Bioorg Med Chem. 2010;18(5):1925-1935.

6. Dilly S, Graulich A, Liegeois JF. Molecular modeling study of 4-phenylpiperazine and 4-phenyl-1,2,3,6-tetrahydropyridine derivatives: a new step towards the design of high-affinity 5-HT1A ligands. Bioorg Med Chem Lett. 2010;20(3):1118-1123.

7. Di Fabio R, Griffante C, Alvaro G, Pentassuglia G, Pizzi DA, Donati D, et al. Discovery process and pharmacological characterization of 2-(S)-(4-fluoro-2-methylphenyl)piperazine-1-carboxylic acid [1-(R)-(3,5-bis-trifluoromethylphenyl)ethyl]methylamide (vestipitant) as a potent, selective, and orally active NK1 receptor antagonist. J Med Chem. 2009;52(10):3238-3247.

8. Neves G, Kliemann M, Betti AH, Conrado DJ, Tasso L, Fraga CA, et al. Serotonergic neurotransmission mediates hypothermia induced by the N-phenylpiperazine antipsychotic prototypes LASSBio-579 and LASSBio-581. Pharmacol Biochem Behav. 2008;89(1):23-30.

9. Weerts A, Pattyn N, Van de Heyning P, Wuyts F. Evaluation of the effects of anti-motion sickness drugs on subjective sleepiness and cognitive performance of healthy males. J Psychopharmacol. 2013;28(7):655-664.

10. Gaginella TS. Serotonin in the intestinal tract: A synopsis. 1st Ed. Gaginella TS, Galligan JJ, editors. New York: CRC Press; 1995.

11. Costedio MM, Hyman N, Mawe GM. Serotonin and its role in colonic function and in gastrointestinal disorders. Dis Colon Rectum. 2007;50(3):376-388.

12. Tsukamoto K, Ariga H, Mantyh C, Pappas TN, Yanagi H, Yamamura T, Takahashi T. Luminally-released serotonin stimulates colonic motility and accelerates colonic transit in rats. Am J Physiol Regul Integr Comp Physiol. 2007;293(1):R64-R69.

13. Haga K, Asano K, Fukuda T, Kobayakawa T. The function of 5-HT3 receptors on colonic transit in rats. Obes Res. 1995;3 (Suppl 5):801S-810S.

14. Borman RA, Burleigh DE. Human colonic mucosa possesses a mixed population of 5-HT receptors. Eur J Pharmacol. 1996;309(3):271-274.

15. Kuramoto H, Kadowaki M, Sakamoto H, Yuasa K, Todo A, Shirai R. Distinct morphology of serotonin-containing enterochromaffin (EC) cells in the rat distal colon. Arch Histol Cytol. 2007;70(4):235-241.

16. Chen JX, Pan H, Rothman TP, Wade PR, Gershon MD. Guinea pig 5-HT transporter: cloning, expression, distribution, and function in intestinal sensory reception. Am J Physiol. 1998;275(3 Pt 1):G433-G448.

17. Ning Y, Zhu JX, Chan HC. Regulation of ion transport by 5-hydroxytryptamine in rat colon. Clin Exp Pharmacol Physiol. 2004;31(7):424-428.

18. Bunce KT, Elswood CJ, Ball MT. Investigation of the 5-hydroxytryptamine receptor mechanism mediating the short-circuit current response in rat colon. Br J Pharmacol. 1991;102(4):811-816.

19. Al-Tabakha MM. Future prospect of insulin inhalation for diabetic patients: The case of Afrezza versus Exubera. J Control Release. 2015;215:25-238.

20. Petersen SB, Nolan G, Maher S, Rahbek UL, Guldbrandt M, Brayden DJ. Evaluation of alkylmaltosides as intestinal permeation enhancers: comparison between rat intestinal mucosal sheets and Caco-2 monolayers. Eur J Pharm Sci. 2012; 47(4):701-712.

21. Hubatsch I, Ragnarsson EG, Artursson P. Determination of drug permeability and prediction of drug absorption in Caco-2 monolayers. Nat. Protoc. 2007;2(9):2111-2119.

22. Feighery LM, Cochrane SW, Quinn T, Baird AW, O'Toole D, Owens SE, O'Donoghue D, Mrsny RJ, Brayden DJ. Myosin light chain kinase inhibition: correction of increased intestinal epithelial permeability in vitro. Pharm Res. 2008;25(6):1377-1386.

23. Yang N, Xue H, Guo H, Chen X, Zhu JX. Segmental heterogeneity of epithelial ion transport induced by stimulants in rat distal colon. Biol Pharm Bull. 2006;29(9):1825-1829.

24. Fowler SB, Poon S, Muff R, Chiti F, Dobson CM, Zurdo J. Rational design of aggregation-resistant bioactive peptides: re-engineering human calcitonin, Proc. Natl. Acad. Sci. U S A. (2005) 102: 10105-10110.

25. Berridge MV, Tan AS. Characterization of the cellular reduction of 3-(4,5-dimethylthiazol-2-yl)-2,5-diphenyltetrazolium bromide (MTT): subcellular localization, substrate dependence, and involvement of mitochondrial electron transport in MTT reduction. Arch. Biochem. Biophys. 1993; 303(2)**:** 474-482.

26. Maher S, Kennelly R, Bzik VA, Baird AW, Wang X, Winter D, Brayden DJ. Evaluation of intestinal absorption enhancement and local mucosal toxicity of two promoters. I. Studies in isolated rat and human colonic mucosae. Eur J Pharm Sci. 2009;38(4):291-300.

27. Briske-Anderson MJ, Finley JW, Newman SM. The influence of culture time and passage number on the morphological and physiological development of Caco-2 cells. Proc. Soc. Exp. Biology Med. 1997;214(3):248-257.

28.Leonard M, Creed E, Brayden D, Baird AW. Evaluation of the Caco-2 monolayer as a model epithelium for iontophoretic transport. Pharm Res. 2000;17(10):1181-1188.

29. Marušić M, Zupančič T, Hribar G, Komel R, Anderluh G, Caserman S. The Caco-2 cell culture model enables sensitive detection of enhanced protein permeability in the presence of N-decyl-β-d-maltopyranoside. Nature Biotechnol. 2013;30(5):507-515.

30. Ungell AL, Nylander S, Bergstrand S, Sjoberg A, Lennernass H (1998). Membrane transport of drugs in different regions of the intestinal tract of the rat. Journal of Pharmaceutical Sciences

1998; 87(3): 360-366.

31. Hamilton MK, Boudry G, Lemay DG, Raybould HE. Changes in intestinal barrier function and gut microbiota in high-fat diet-fed rats are dynamic and region dependent. Am J Physiol Gastrointest Liver Physiol. 2015;308(10):G840-G851.

32. Feighery L, Smyth A, Keely S, Baird AW, O'Connor WT, Callanan JJ, Brayden DJ. Increased intestinal permeability in rats subjected to traumatic frontal lobe percussion brain injury.J Trauma 2008; 64(1):131-137.

33. Gill RK, Saksena S, Tyagi S, Alrefai WA, Malakooti J, Sarwar Z, et al. Serotonin inhibits Na+/H+ exchange activity via 5-HT_4 receptors and activation of PKC alpha in human intestinal epithelial cells. Gastroenterology 2005;128(4):962-974.

34. Alcalde AI, Sorribas V, Rodriguez-Yoldi MJ, Lahuerta A. Study of serotonin interactions with brush border membrane of rabbit jejunum enterocytes. Eur J Pharmacol 2000;403(1-2):9-15.

35. Karczewski J, Groot J. Molecular physiology and pathophysiology of tight junctions III. Tight junction regulation by intracellular messengers: differences in response within and between epithelia. Am J Physiol Gastrointest Liver Physiol. 2000;279(4):G660-G665.

36. Nagatsu T, Suzuki H, Kiuchi K, Saitoh M, Hidaka H. Effects of myosin light-chain kinase inhibitor on catecholamine secretion from rat pheochromocytoma PC12h cells. Biochem Biophys Res Commun. 1987;143(3):1045-1048.

37. Denizot J, Sivignon A, Barreau F, Darcha C, Chan HF, Stanners CP, Hofman P, Darfeuille-Michaud A, Barnich N. Adherent-invasive *Escherichia coli* induce claudin-2 expression and barrier defect in CEABAC10 mice and crohn's disease patients. Inflamm Bowel Dis. 2012;

18(2):294-304.

38. Aguirre TA, Teijeiro-Osorio D, Rosa M, Coulter IS, Alonso MJ, Brayden DJ. Current status of selected oral peptide technologies in advanced preclinical development and in clinical trials. Adv Drug Deliv Rev. 2016; Feb 24. pii: S0169-409X(16)30055-2. doi: 10.1016.

Figure Legends

Fig. 1. Structure of 1-phenyl piperazine (PPZ)

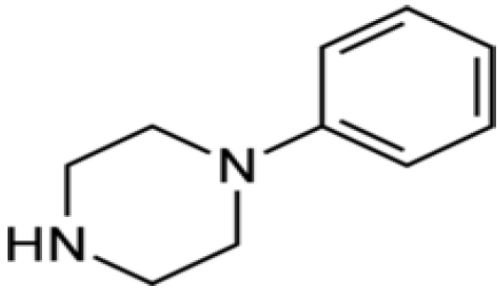

Fig. 1

Fig. 2. The effect of apical addition of PPZ on Papp of (a) [^{14}C]-mannitol, (b) FD-4, (c) FD-40, (d) FD-70 across Caco-2 monolayers over 120 min. (e) Reduction in TEER following apical addition of PPZ across monolayers at time zero. N= 3-12 per group or concentration. *P<0.05; **P<0.01; ***P<0.001, compared to untreated controls.

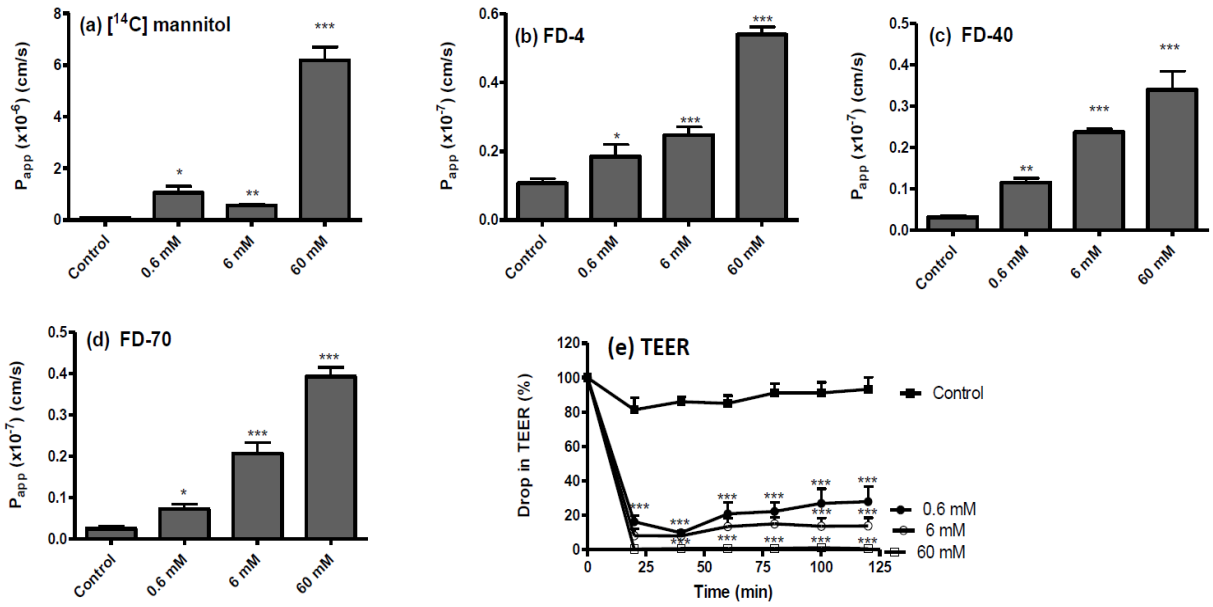

Fig. 3. The effect of apically-added PPZ (n=3 for each concentration) on the Papp of [^{14}C]-mannitol and FD-4 over 120 min across (a) ileal and (b) distal colonic mucosae. *P<0.05; **P<0.01; ***P<0.001, compared to basal Papp of [^{14}C]-mannitol or FD-4 respectively. N=4-10 ileal and colonic tissues. (c) PPZ induces a decrease in TEER in ileal mucosae and (d) colonic mucosae. ***P<0.001, compared to TEER of untreated tissue. N= 4 at each concentration. PPZ added at time zero in (c) and (d).

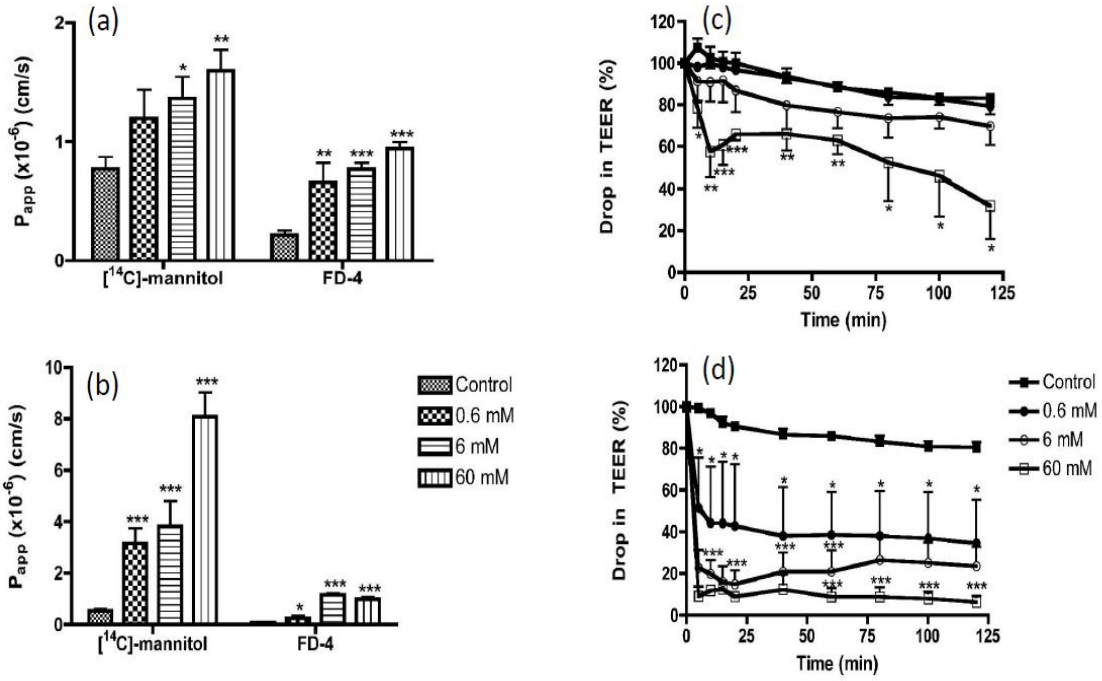

Fig. 3

Fig. 4. TEER recovery in Caco-2 monolayers following 2h exposure to PPZ at time zero, subsequent wash-out, and incubation in fresh buffer over 24 h in DMEM. ***P<0.001, compared to untreated controls at 2 h; ***P<0.001, for monolayer treated with 60 mM PPZ compared to untreated controls at 24 h (n=4)

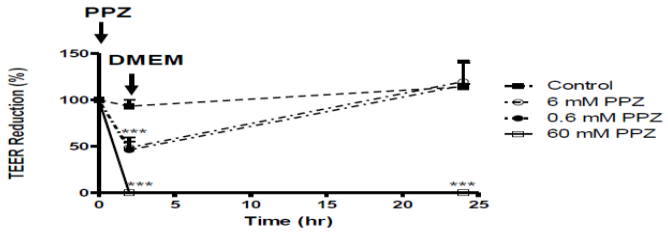

Fig. 4

Fig. 5. The effect of 5-HT_4 antagonists on PPZ-induced Papp of [^{14}C]-mannitol. 20 min pre-treatment with SB-204070 (SB; 10 µM) and GR11808 (GR; 1 µM) followed by PPZ. (a) Caco-2 monolayers: *** P<0.01 comparing 0.6 mM PPZ in the presence and absence of inhibitors, and also for PPZ versus untreated controls (b) rat colonic mucosae: *P<0.05; compared to PPZ at three respective concentrations without antagonists; **P< 0.01 for PPZ compared to untreated controls (n=4-12).

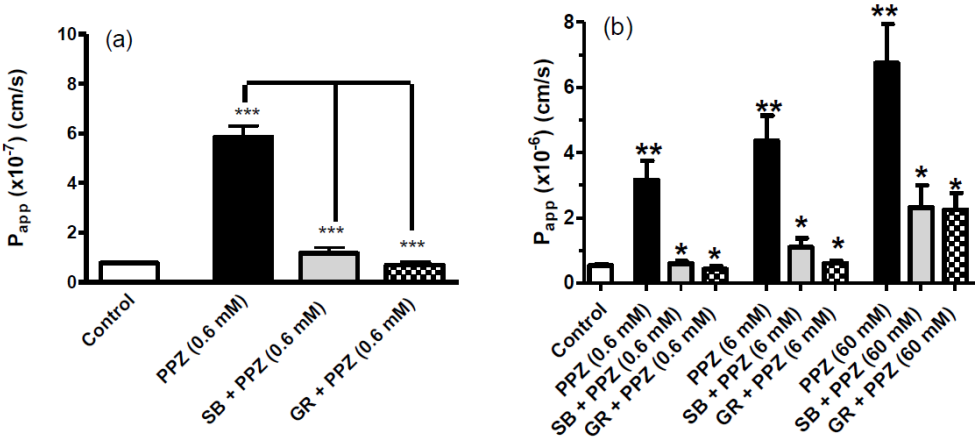

Fig. 5

Fig. 6. Release of cAMP (expressed as % maximum) of PPZ-treated (0.6-60 mM) (a) Caco-2 cells and (b) rat distal colonic mucosae for 20 min, compared to FSK (10µM) control. *P<0.05; **P<0.01; ***P<0.001 (n=4 each group). (c) PPZ increased Isc across colonic mucosae predominantly from the apical side (n=3 for each concentration).

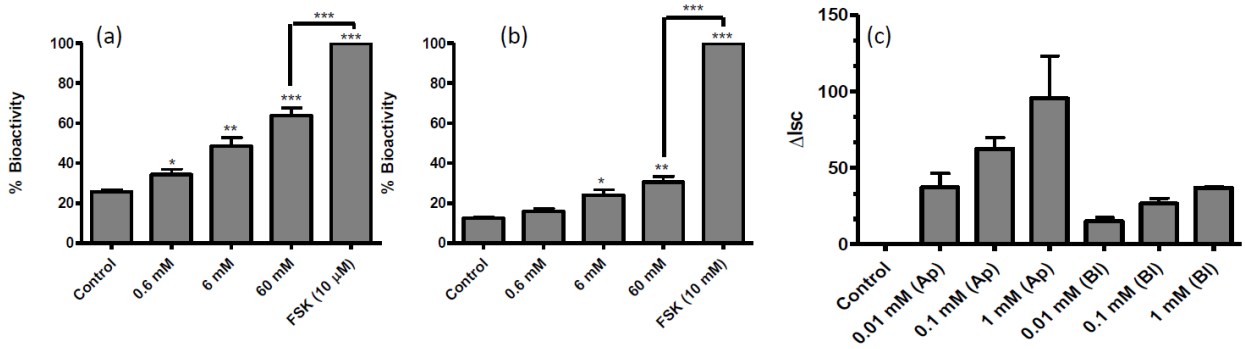

Fig. 6

Fig. 7. The effect on Papp values of [^{14}C]-mannitol and FD-4 by pre-incubation of ML9 (10 µM) on PPZ-induced permeability in (a) Caco-2 monolayers and (b) rat colonic mucosae. Symbol codes are the same for a, b. *P<0.05; **P<0.01; ***P<0.001, compared to controls (n=4, each group).

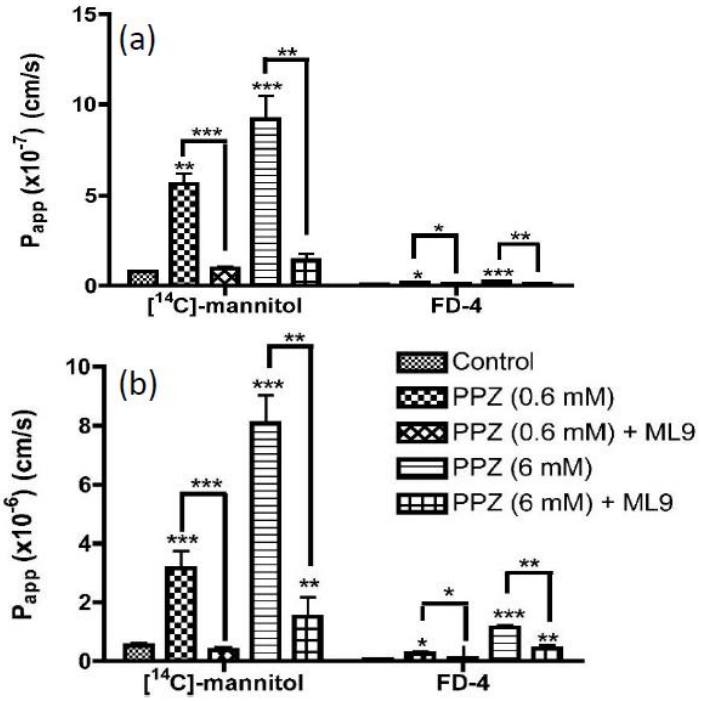

Fig. 7

Fig. 8. Confocal images of Caco-2 monolayers (a) control [F-actin (green) and DAPI staining (blue)]; (b) PPZ (0.6 mM) for 20 min [F-actin (green) and DAPI staining (blue)]; (c) Control [claudin-2 (red), F-actin (green) and DAPI staining (blue)] and (d) PPZ (0.6 mM) for 20 min [claudin-2 (red), F-actin (green) and DAPI staining (blue). Bars =20 µm).

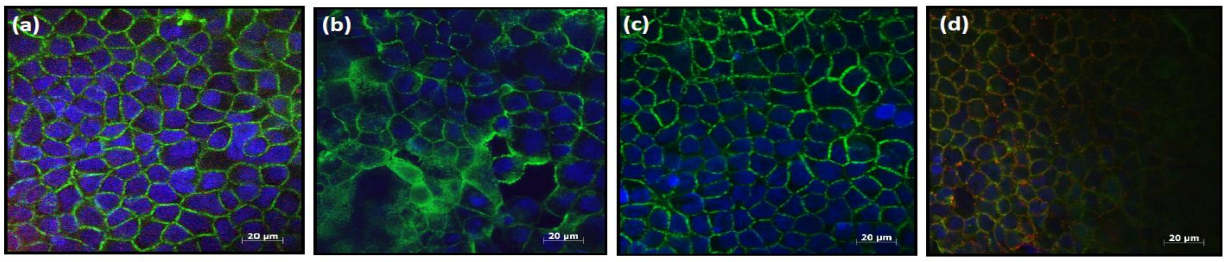

Fig 8

Fig. 9. MTT assay of (a) Caco-2 cells treated with PPZ (60 µm-60 mM) or Triton® X-100 (0.1% v/v after 1 h and (b) 24 h. **P<0.01; ***P<0.001, compared to media control (n=3). LDH release from (c) ileal and (d) colonic mucosae treated with three concentrations of PPZ for 120 min. Values were referenced to maximal values seen in response to exposure to Triton® X-100 (10% v/v) and were compared to untreated controls. **P<0.01; ***P<0.001 (n=3-4 per group).

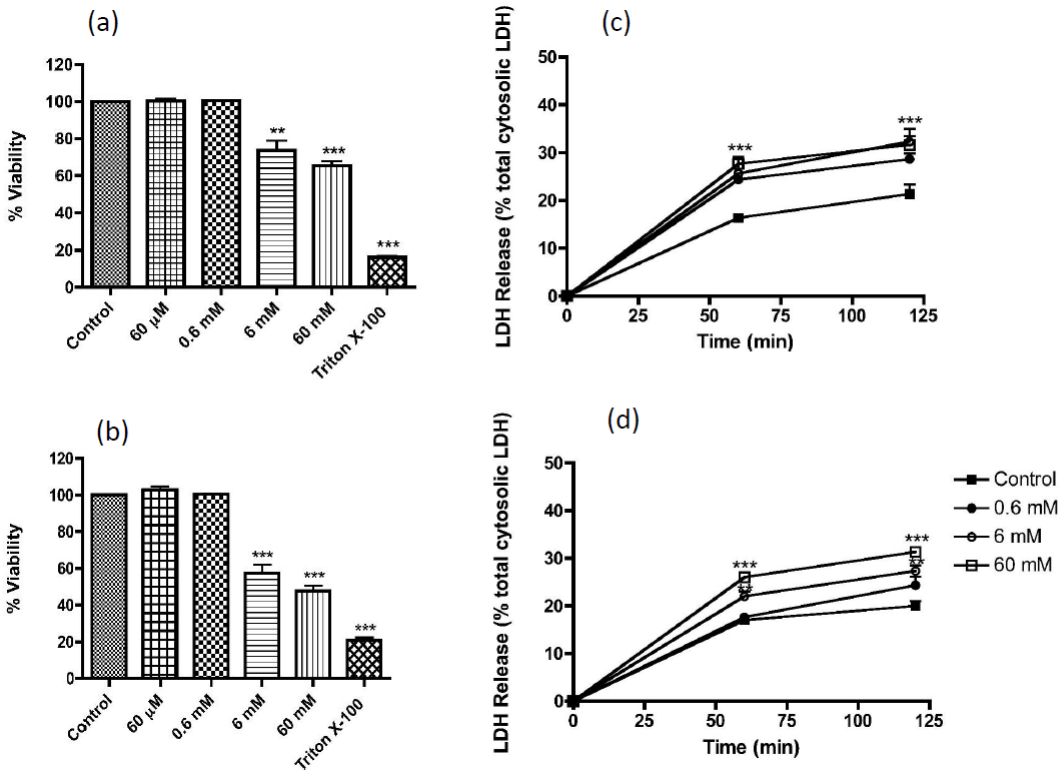

Fig 9

Fig. 10. H & E stained light micrographs of rat intestinal mucosae mounted in Ussing chambers and exposed to PPZ for 120 min. Ileum: (a) untreated; (b) 0.6 mM PPZ; (c) 6 mM PPZ. Colon: (d) untreated; (e) 0.6 mM PPZ; (f) 6 mM PPZ (Bar=10 µm).

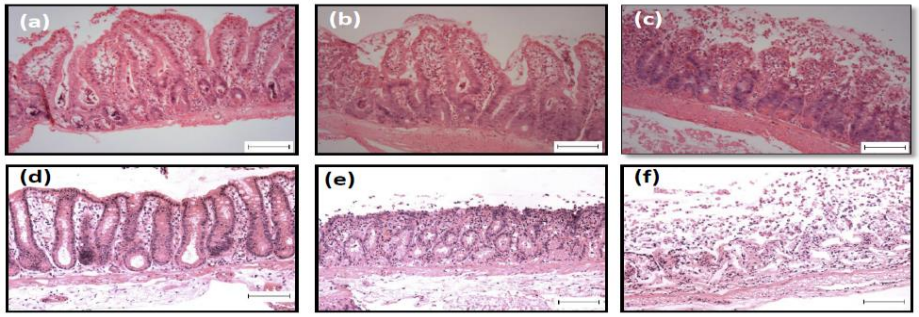

Fig 10

Fig. 11. Cartoon of likely mechanism of action of PPZ in intestinal tissue mucosae. Na/K/2Cl is the cotransporter and CFTR is the cystic fibrosis transmembrane regulator. Activation of the combination of two transporters by PPZ-stimulation of intracellular cAMP via apical $5HT_4$ receptors gives rise to an increase in electrogenic chloride secretion (increase in Isc) and tight junction (TJ) opening in parallel. Indirect Na/K/2Cl activation by PPZ also leads to tight junction opening since the effects of PPZ on paracellular flux were inhibited by bumetanide. Piperazine structures also induce an alkaline pH in the apical buffer, which may impact on permeability (3).

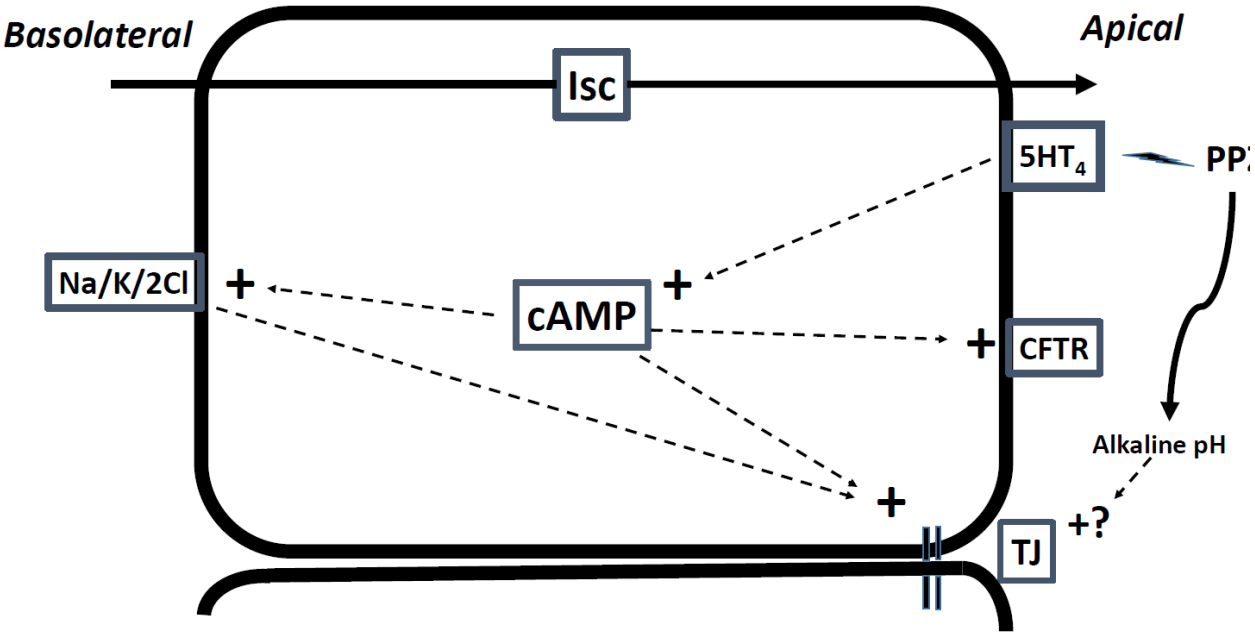

Fig. 11

583

584 **Table 1.** Pretreatment with basolateral addition of bumetanide for 20 min prior to apical
585 addition of PPZ reduces the stimulation of the P_{app} of [^{14}C]-mannitol across distal colonic
586 mucosae at 120 min. **P<0.05; **P<0.01, compared to PPZ alone. PPZ alone increased the
587 Papp (P<0.001) at each concentration versus control. **P<0.05; **P<0.01, compared to PPZ
588 alone. PPZ alone increased the Papp (P<0.001) at each concentration versus control.

PPZ (mM)	**Mannitol P_{app} (10^{-6} (cm/s))**	**Mannitol P_{app} (10^{-6} (cm/s)) in presence of bumetanide (100µM)** 589 590
0	0.5 ± 0.1 (n=9)	0.5 ± 0.2 (n=3)
0.6	3.2 ± 0.6 (n=14)	0.5 ± 0.1 ** (n=4)
6	3.8 ± 1.0 (n=4)	1.9 ± 1.1 (n=4)
60	6.8 ± 1.2 (n=4)	2.7 ± 0.3* (n=4)